

Two Stage Adaptive Histogram Valley based Thresholding for Tumor Extraction in Brain MRI Images

Shrikant Burje¹, Sourabh Rungta^{2*}, Anupam Shukla³

¹ PhD Scholar, Electronics & Communication, Rungta College of Engineering and Technology, Bhilai, INDIA

² Professor, Rungta College of Engineering and Technology, Bhilai, INDIA

³ Director, IIIT Pune, Maharashtra, INDIA

ABSTRACT

Detection of brain tumors is a delicate aspect as far as research is concerned in the field of medical engineering. The prerequisite of removing tumors from human brain is to accurately identify the affected area of interest. Being the central processing unit of the human body any micro harm to any portion of the brain can either put the subject to miserable conditions or may be a reason for the cause of death. The work in this paper is concerned in accurately detecting the non-functional cells called tumor in human brain. A six-stage process based on two level wavelet decomposition and local and global adaptive thresholding based on histogram decomposition is used. A global threshold is then calculated using the average value of all six threshold values and the reconstructed image is once again applied for global thresholding. 77 normal and 70 affected images were considered for this work and the results were validated with the ground truth. The performance was accurate for all the images considered for this work. Inhomogeneous and negative illumination to hard and soft tissues in other images not considered in this work results in over and under segmentation.

Article Received: 10 August 2020, Revised: 25 October 2020, Accepted: 18 November 2020

Introduction

A mass of abnormal cells tends to grow at faster rate to form a Brain Tumor. Depending on the type of tumor whether benign or malignant, these tumors grow over a changing period of time inside the skull and creates a pressure due to closed space thus giving rise to various symptoms. The Benign are curable and can be destroyed since the rate of growth is slow whereas malignant are difficult to handle and cannot be removed completely which ranges from grade I to grade IV. Grade IV tumors are the most severe types and are the reason for person death. Diagnosing brain tumors ahead of time and being severe becomes important since they become life threatening. They find eight and fifth place in common cancers among males and females with age group of 40-59 respectively. The most common types of cancers found in adults are Meningiomas and Gliomas. The percentage of children and younger people affected by such dangerous disease is relatively low as compared to the adults but the survival rate is higher than the adults for all types of brain tumor.

The major challenge in treatment of tumors rely on accurate diagnosis of its type which ranges from a low grade to aggressive one. Cancer grades are used to determine prognosis, and assist in treatment planning. Determining the type of tumor

is a method which rely upon invasive surgical techniques to obtain tissue samples, which is a high-risk process and anxiety-provoking for subjects under treatment. Recently, article published in Nature Medicine describe a non-invasive and easy technique for the classification of tumors on 22, June 2020. Some of the tumors may be small enough to be treated without a surgery. Safe and successful treatment of brain lesions depend on the exact detection of the region of interest which has to be surgically removed using either radiosurgery, radiation therapy or targeted therapy.

Many researchers have proposed variety of techniques for the detection of tumor part of the brain. A wavelet-based feature extraction is suggested in [1]. They extracted the tumor region using thresholding and separated the non-tumor part. Support vector Machine (SVM) was trained with the features provided from tumor and non-tumor part of the brain region. A similar approach using SVM has been identified in [2] where the authors used feature set for every applicant lesion using shape, texture, and intensity. Binarization using Otsu and then segmentation by K-means was proposed in [3]. They used DWT followed by PCA for feature extraction and SVM to classify the MRI images. A simple and low complexity U-Net model (Fully Convolutional Network) (FCN) for tumor segmentation has been listed in [4]

where class weights were used instead of pixel weight maps. A similar approach was used in [5] where the author used CNN with randomly selected patch wise samples from the affected and non-affected regions to train the classifier. Work proposed in [6] used texture and statistical based features for training six different classifiers and concluded that CNN outperformed others. Fuzzy C-means clustering approach was incorporated for segmenting the affected region of the brain. In [7], features from tumor region based on 2-D DWT and Gabor filters were combined to train a feed forward network. The tumor segmentation part was done manually. The research presented in [8] used a new CNN for classification of three different types of brain tumor which was tested on T1-weighted contrast enhanced MRI images. Using 10-fold cross validation on two datasets they obtained an accuracy of approximately 96%. A different set of advanced higher order statistical features [9] was extracted from the ROI of brain and classified using SVM. The work proposed was able to locate tumor tissues based on a single spectral structural MRI. High computational cost and memory requirement was optimized using U-Net with adaptive thresholding to segment the ROI of tumor in [10]. The authors applied their technique on 3064 images with three types of tumor and estimated the performance using recall and dice similarity metrics and found that their method outperforms with respect to training time with other methods. Early stage multiple tumor detection regardless of inhomogeneity of intensity, dimensions and spatial location were handled using automated machine vision technique in [11]. The technique comprised of clustering based on K-means, patch-based processing and counting of objects in the MRI images. Muhammad Sharif et. al. The authors in [12] proposed tumor detection technique based on extreme learning machine (ELM). MRI images from BRATS 2012-2015 datasets and 2013 Leader board which were enhanced using triangular Fuzzy median filtering and segmented using unsupervised fuzzy set. Texture features were extracted using Gabor and applied to ELM and regression ELM was capable to extract the tumor.

Features based on GLCM and textures were classified using SVM and ANN in [13]. Otsu thresholding technique was used to segment the tumor region. The work in [13] showed that ANN

worked superior with respect to SVM for 20 regular and 140 abnormal axial plane T2-weighted MR brain images. K-means with SVM was proposed in [14] with binary thresholding. Hierarchical CNN [15] to exploit local and global contextual features for low- and high-grade glioblastoma was proposed for handling diverse tumor in terms of shape, size, location and overlapping tissues. Experimental results over 400 brain MRI images showed low time complexity with respect to other state of art techniques. Ahmet Çinar and Muhammed Yildirim in [16] proposed a modified Resnet50 architecture-based CNN model. They removed last 5 layers of the model and added eight new layers for experimenting on KAGGLE dataset consisting of 98 normal and 155 affected images. They compared the ground truth with other architecture such as Alexnet, Resnet50, InceptionV3, GoogleNet and Densenet201 models and concluded that their proposed modified CNN model outperformed in terms of accuracy. Deep learning approaches related to brain tumor analysis can be found in [17]. The detailed study focuses on taxonomy and future challenges in tumor detection and classification in MRI images. The paper is organised in VI stages for the novel technique followed by results and conclusions. The stages involve: Pre-processing, Wavelet decomposition (Level 1 and 2), Adaptive thresholding, Wavelet reconstruction, Global thresholding and filtering.

Proposed Methodology

All papers

Brain tumor detection process involves six stages: Preprocessing, Wavelet decomposition and analysis, thresholding wavelet coefficients using adaptive threshold from 1 dimensional wavelet decomposition to histograms obtained from wavelet higher components, Reconstruction, Global Adaptive thresholding and filtering the resultant image after reconstruction. Many wavelet families are included in MATLAB wavelet toolbox such as Haar, Coieflets, Symlets, Debauchees etc with numbers of mother wavelets in each of the family. Debauchees 6 mother wavelet was selected based on experimental results since other mother wavelets when applied for the analysis showed poor performance with respect to poor segmentation and misclassification due to various reasons. The reasons include differentiated illumination from other images of

the groups (Normal and Affected), high illumination for the hard tissues than the tumor region and negative illumination with respect to tumor region and other parts of the brain (tumor being darker and other brain tissues being brighter). The number of images not considered due to above facts were 14 Normal and 57 Affected whereas all 77 Normal and 70 Affected were successfully read, detected and segmented by the proposed system from a set of 91 normal and 127 affected images considered for this work. All the images were obtained from KAGGLE dataset. One single image (Affected) was not considered due to its incorrect image format.

STAGE I: Pre-processing

In the first stage, the image is read and converted to grayscale image as shown in figure 1. The KAGGLE dataset images vary with respect to the height and width, so to maintain uniformity in height and width of each image, the images were resized to height H=256 and width W=256. The values of H and W was so selected to ensure that there will be negligible loss of features since almost all the images height and width was above the defined values. The resizing not only maintained the size uniformity but also reduced computational and time complexity. Further for better ROI (Region of interest) extraction, contrast stretching was applied with default parameters. A prior view was obtained about the distribution of pixel values(intensity) over the intensity range of the image which is indicated in figure 2 below.

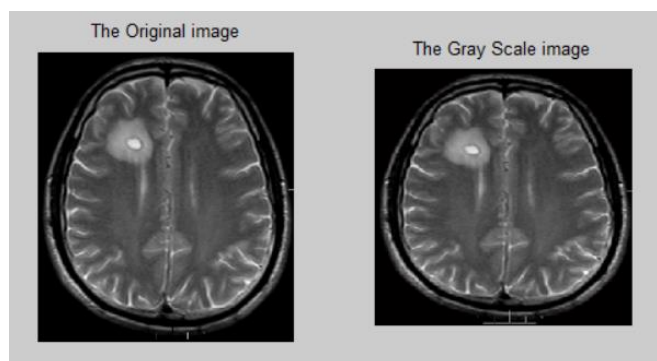


Fig.1. – Original input image and its grayscale image resized to [256 256]

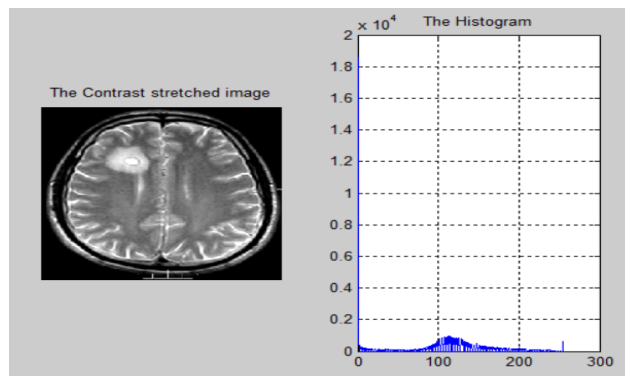


Fig. 2. – Image after contrast stretching and its histogram

STAGE 2: Wavelet Decomposition

Level 1 –

The above histogram of the image does not show a clear-cut value for separating the tumor part from the image therefore finding proper value of threshold was necessary. For the purpose, the grayscale image was down sampled using wavelet decomposition (db6 as Mother wavelet). The four components thus obtained were A1, H1, V1 and D1 respectively corresponding to approximation, horizontal, vertical and detail component as shown in figure 3 and 4.

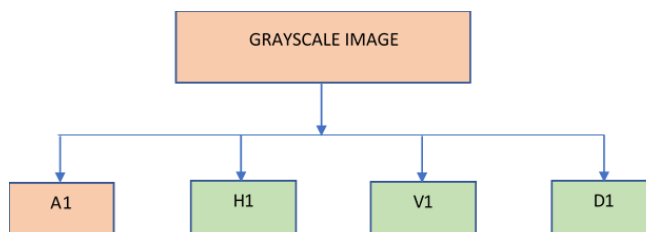


Fig.3. – 2D wavelet transform at level 1. A1, H1, V1 and D1 representing the Approximation, Horizontal, Vertical and Detail components of the transform using mother wavelet db6.

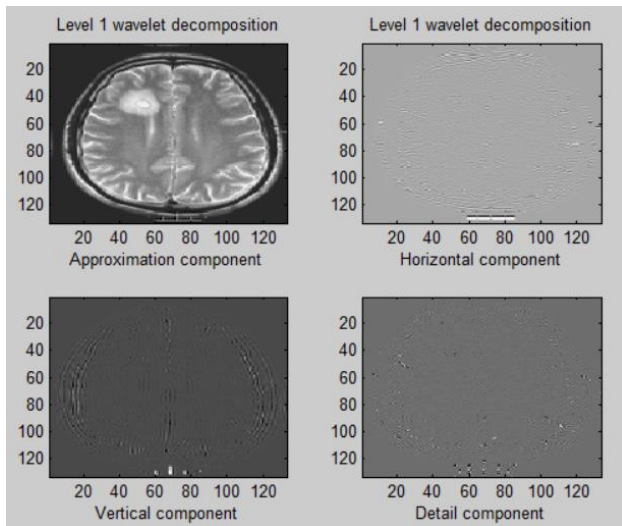


Fig.4. – Approximation, Horizontal, Vertical and the detail components after 1st level of wavelet decomposition using mother wavelet db6

Histograms for H1, V1 and D1 was obtained after transforming the wavelet coefficients of these components in the intensity range of [0 255]. The transformation process involves the following steps as indicated in Algorithm 1:

1. Find the minimum value from the component (say C). (Most probably a negative value due to wavelet decomposition)

$$Mn = \min [C] \tag{1}$$

2. Add the absolute value of the minimum value to all values in the component so that the minimum value of the component will be zero. As a result, the maximum value of the component will definitely increase.

$$S = [C] + \text{abs} (Mn) \tag{2}$$

3. Now find the maximum value in the component and divide all values by the maximum value so that the range of the values falls in the interval [0 1]

$$R = \frac{S}{Mx = \max [S]} \tag{3}$$

4. Multiply the values by 255 and roundup all the values so that the obtained integer values include the decimal part. Convert the values as unsigned integers.

$$T = \text{round} (R * 255) \tag{4}$$

Finally, the histograms are obtained for all the three components after transformation of the wavelet coefficients as above. The 1-dimensional array or row vector representing the histogram values for each of the three components were then decomposed to level 5 using the same mother wavelet as shown in figure 5.

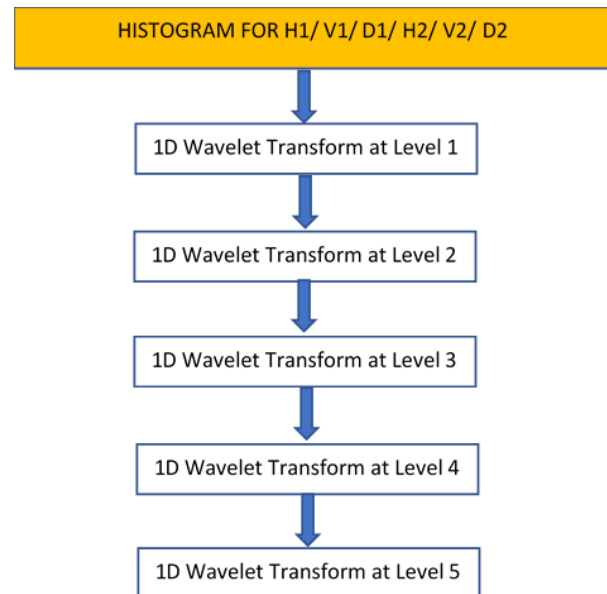


Fig.5. – 1D wavelet transform up to level 5 for finding the THRESHOLD corresponding to GLOBAL minima.

After obtaining the level 5 components of the 256-length vector, the point for Global Minima was searched. Level 5 was experimentally decided since at this stage high frequencies were eliminated and the Global Minima point was then used to find the threshold value in the component histogram of 256 values. Let us say that at level 5, the number of samples are $S_n=8$ and the Global Minima is found at point $G_m=3$. Then the threshold point in $H_n=256$ samples representing the component histogram was:

$$Tx = \frac{Hn * Gm}{Sn} \tag{5}$$

Threshold corresponding to all three components except the approximation component is evaluated in similar way resulting in three thresholds Th_1 , Tv_1 and Td_1 respectively for horizontal, vertical and detail components. The figures 6-8 below show the 1D wavelet decomposition of histograms

for the three components up to level 5 using the same mother wavelet db6.

Figure 8 – Histogram of 1st level 1D wavelet decomposition for Diagonal component and detail coefficients plot from level 1 to 5 decomposition

Level 2 –

A similar approach is carried out as mentioned above in STAGE 2, Level 1 part for the decomposition components at level 2. The approximation component at level 1 i.e. CA1 is again decomposed and wavelet components at this level are obtained as A2, H2, V2 and D2 respectively as indicated in figure 9 and 10.

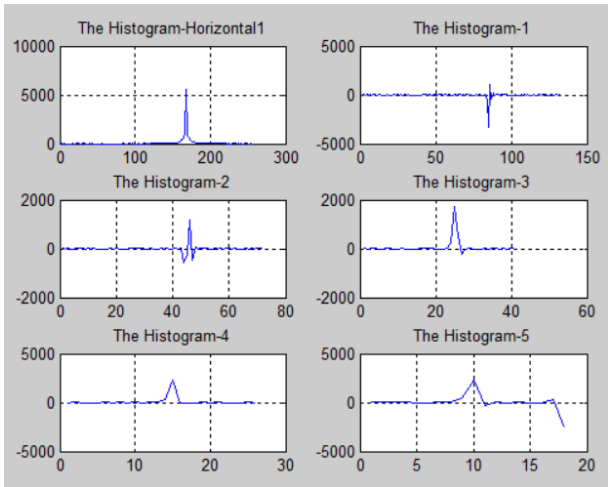


Fig.6. – Histogram of 1st level 1D wavelet decomposition for Horizontal component and detail coefficients plot from level 1 to 5 decomposition

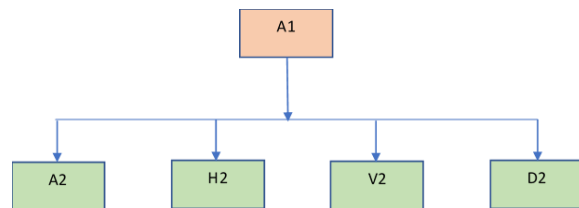


Figure 9 – 2D wavelet transform at level 2. A2, H2, V2 and D2 representing the Approximation, Horizontal, Vertical and Detail components of the transform using mother wavelet db6.

The wavelet coefficients of H2, V2 and D2 are transformed and converted to unsigned integers as listed in steps above and three new thresholds are gained for this level as Th2, Tv2 and Td2 respectively for H2, V2 and D2 level 2 wavelet components.

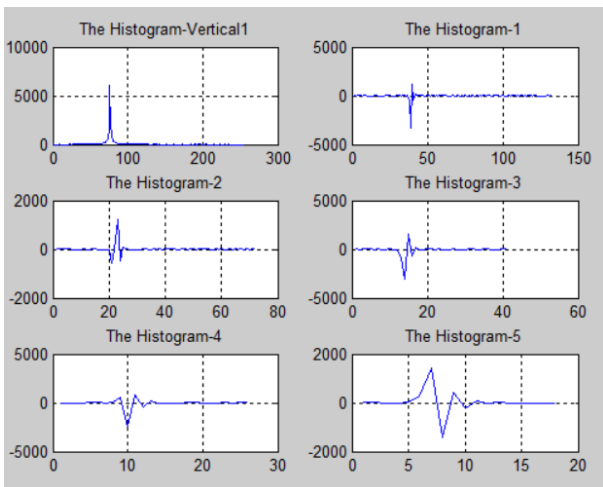


Fig.7. – Histogram of 1st level 1D wavelet decomposition for Vertical component and detail coefficients plot from level 1 to 5 decomposition

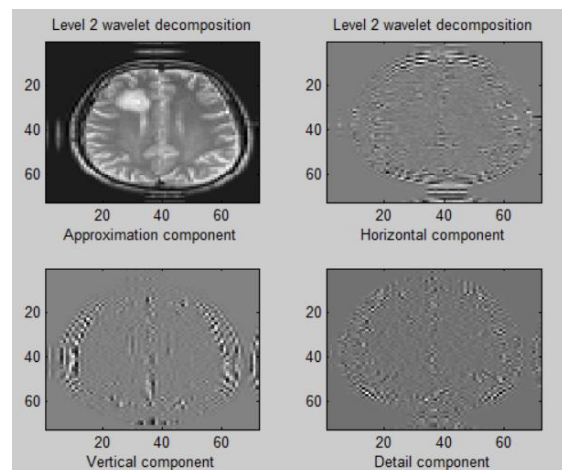


Fig.10. – Approximation, Horizontal, Vertical and the detail components after 2nd level of wavelet decomposition using mother wavelet db6.

Further decomposition and finding threshold do not showed improvement over the segmentation results. Experiments were carried up to 5 level

decomposition and their respective threshold were evaluated. But it just increased time and computational complexity with negligible gain over the segmentation. Parameters at level 2 decomposition were sufficient to extract the tumor part or the ROI at this stage. Figure 11-13 shows the plots for detail coefficients after 1D wavelet decomposition of the histograms obtained for three components except the approximation component at level 2.

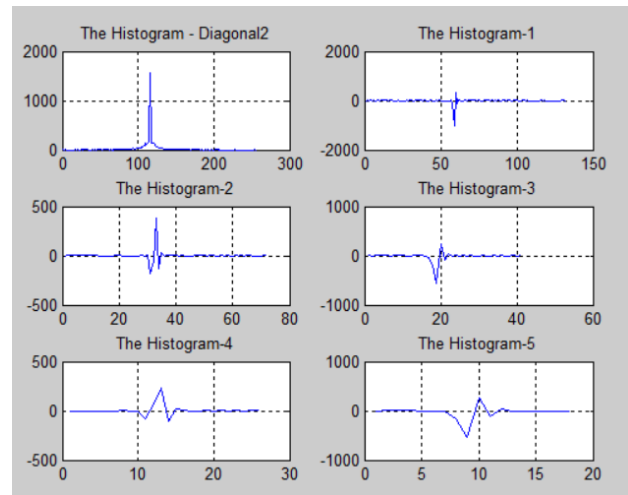


Fig.13. – Histogram of 2nd level 1D wavelet decomposition for Detail component and detail coefficients plot from level 1 to 5 decomposition

STAGE III: Thresholding with Adaptive Thresholds

After calculating six thresholds for all components at level 1 and 2 except for the approximation components, the individual wavelet components were applied with the threshold values and new wavelet components were generated as listed below.

$$C_{new} = \begin{cases} 0, & C_{old} < T_x \\ C_{old}, & C_{old} \geq T_x \end{cases} \quad (6)$$

Thus, the new components generated were H1n, V1n and D1n at level 1 and H2n, V2n and D2n at level 2 respectively.

STAGE IV: Reconstruction

The reconstruction part involves combining all components (H2n, V2n, D2n and A2) at level 2 using inverse wavelet transform using db6 mother wavelet. The resultant component thus obtained is A1n. Note that the approximation component at level 2 that is CA2 is the original component at level 2 and had not undergone any operation to secure the contents of the image. In a similar way, reconstruction at level 1 is achieved using the new component A1n in place of A1 and the operated components at level 1 that are H1n, V1n and D1n respectively. The inverse wavelet transforms at this stage using A1n, H1n, V1n and D1n will yield CAn as the reconstructed component. So, a new image CAn will appear as a replacement to

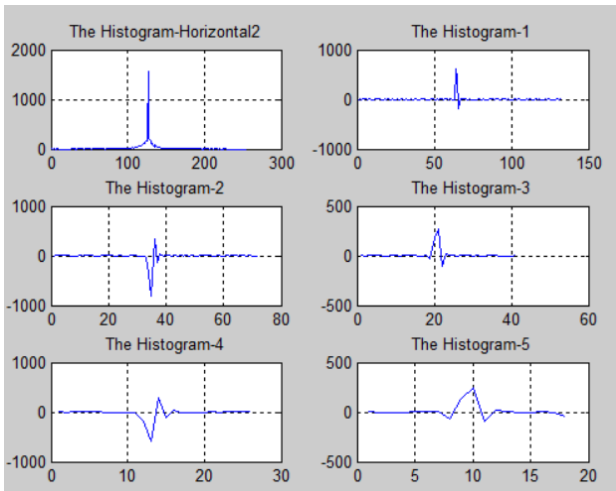


Fig.11. – Histogram of 2nd level 1D wavelet decomposition for Horizontal component and detail coefficients plot from level 1 to 5 decomposition

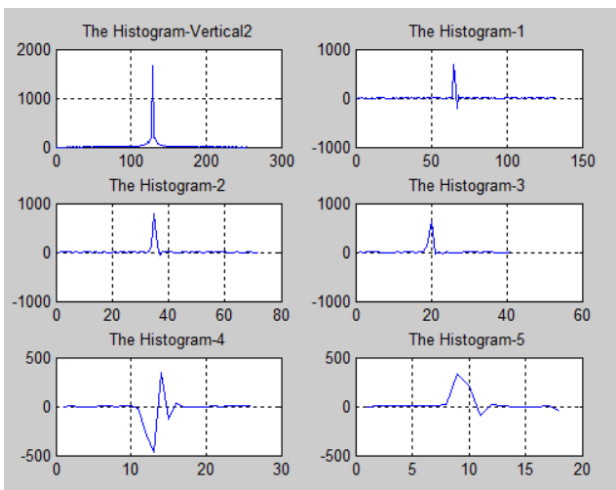


Fig.12. – Histogram of 2nd level 1D wavelet decomposition for Vertical component and detail coefficients plot from level 1 to 5 decomposition

the original image. Stage IV outputs are shown in figure 14 below at both the reconstruction levels.

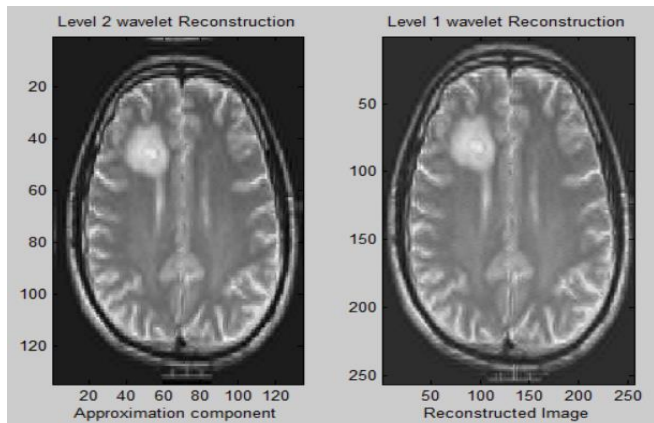


Fig.14.– Reconstructed Approximation component from level 2 components and Reconstructed image after level 1 reconstruction.

STAGE V: Global Adaptive Thresholding

This stage is to fine tuning of the pixels to remove some unwanted pixels from the resultant image which may misclassify the boundaries of the ROI region. The global adaptive threshold T is found simply by taking the mean of all six thresholds values obtained above at level 1 and 2 respectively. Finally, the resultant image (C_{An}) shown in the figure 15 (second image) is applied to this threshold value T to get the final image F (Shown as third image).

$$F = \begin{cases} 0, & C_{An} < T \\ 1, & C_{An} \geq T \end{cases} \quad (7)$$

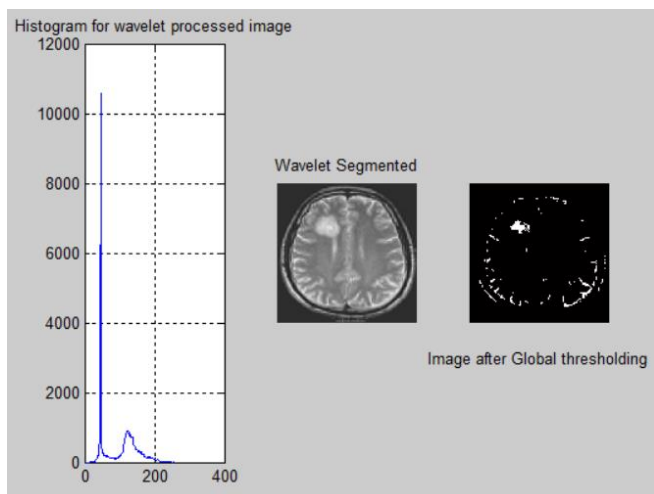


Fig.15. – Histogram for the final image after wavelet-based segmentation and image obtained after the application of Global threshold.

Here the histogram in figure 15 provides a clear indication that the boundaries are separated by means of a valley between two regions that is the background and the ROI. The last segmented image after Global thresholding shows misclassification and thus many small regions belonging to hard tissues are also segmented along with the ROI.

STAGE VI: Filtering and Dimension adjustment

At this stage, the result from most of the images specially for normal images, it showed that some part of hard tissues gets extracted as they seem to be brighter in illumination but their density is small as compared to abnormal region in the affected images. In order to tackle such issues, a filtration operation is performed over the image obtained in the stage VI. A block size of $W_s=15 \times W_s=15$ is considered around each pixel with a threshold value set to

$$T_s = \frac{W_s * W_s}{2} \quad (8)$$

So, for 225 pixels the threshold set was around 112. If the pixel value corresponds to 1 and the total sum of pixel value inside the block or window of 15×15 is greater than 112 then the pixel was marked as tumor pixel otherwise it was marked as non-tumor pixel.

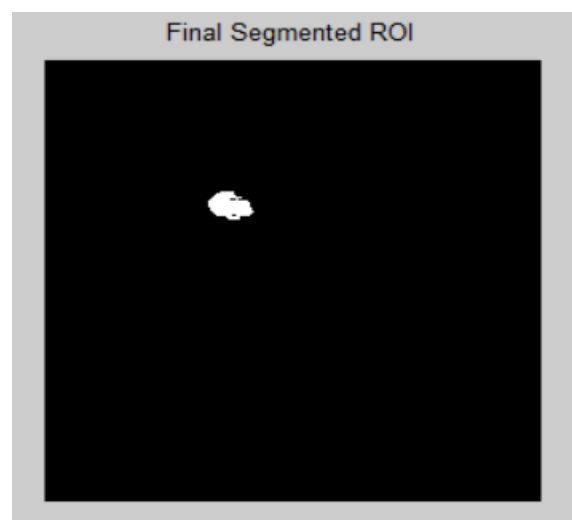


Fig.16. – The final segmented image showing the tumor region after filtering with 15×15 window

To maintain the original size of the image, dimension adjustment was performed by adding sufficient rows and columns to the resultant image. There was loss of rows and columns in the reconstruction process with mother wavelet debauchees 6. This was done to validate the result obtained with the proposed system. The final ROI is indicated in figure 16 as shown above.

Result and Conclusion

The proposed system incorporating six stage segmentation process was successful in extracting the tumor region from the affected images and displaying none for all normal images. The output for a sample normal image is shown below in figure 17 and for the affected image is shown in figure 18. All the 77 normal images and 70 affected images were successfully detected by the system.

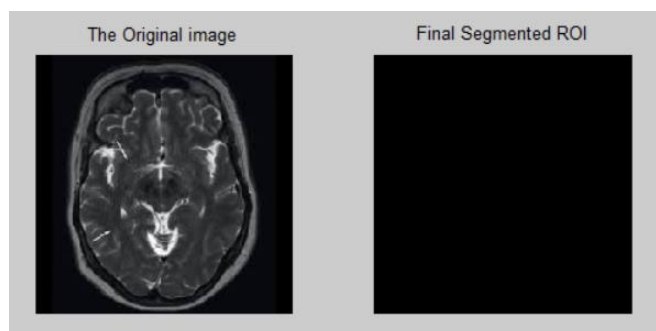


Fig.17. – The resultant segmented image showing none for a Normal image

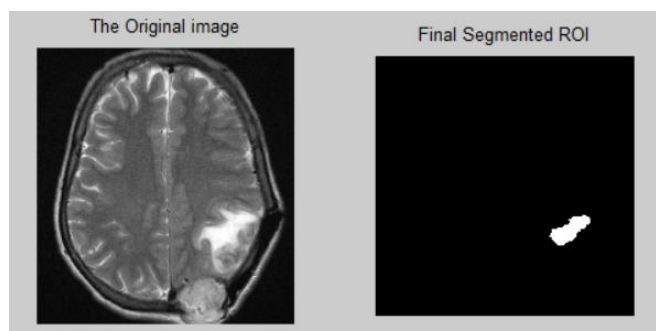


Fig.18. – The resultant segmented image showing ROI for an Affected image

The first image is the original image with different dimensions along rows and columns larger than 256x256 while the segmented image is of [256 256] therefore the extracted part seems to be smaller than the actual. The proposed system was unable to correctly locate the tumor region for

Images similar to figure 19 where the ROI part is non-solid with respect to its illumination or intensity value. A better approach to handle such situation is found in [18]. The other reason is the intensity values of the pixels of the ROI which have lower values as compared to the hard tissues confirmed at the boundaries of the brain.



Fig.19. – Hollow Tumor region with variable intensity across its region.

The drawback of the proposed six stage segmentation system is the dependency on homogeneity of the intensity values for affected and non-affected regions. Also, some tumors small in size may miss due to filtering process where the window size is assumed to be 15x15. Changing the filter window size can detect variable sized tumors but lowering the window size to a small value also detects white spots not defined to ROI from rest of the unaffected region. This can be overcome by inserting robust preprocessing steps at the initial stage. The window size was thus set to 15x15 to avoid over-segmentation in Normal images since in most of the normal images the illumination is not homogeneous and some soft tissues tends to be comparatively brighter than others showing tumor like characteristics. As a result, all the normal images were correctly segmented, that is they showed no single pixels in the segmented output. Some of the normal and affected images not considered due to illumination problems are shown below in the figure 20 and 21 respectively.

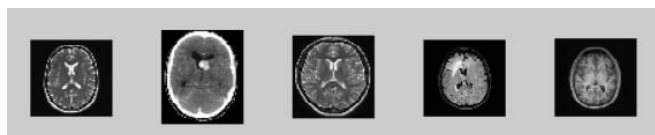


Fig.20. – *Illumination problem with Normal images*

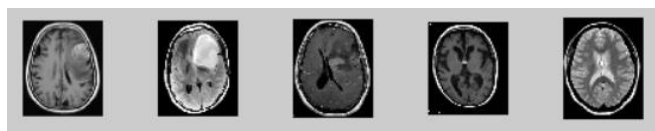


Fig.21. – *Illumination problem with Affected images*

The future work involves in achieving proper illumination corrections to the input images so that more images from different datasets can be taken into consideration. The global threshold is calculated using mean of all thresholds from level 1 and level 2 decompositions for all three components except the approximation component. A more robust formulae for the global threshold can be devised so as to produce accurate results from large number of brain images. The filter window size can be adaptive so as to detect the least possible tumor to large tumors without affecting to the normal images. Histogram processing causes loss of details while transformation of signed real values of wavelet coefficients to unsigned integers as listed in algorithm 1. Another transformation technique with minimum loss can be considered for converting the values. Other mother wavelets or customized mother wavelet can be used for improved results.

References

- [1] Shrikant Burje, Sourabh Rungta and Anupam Shukla, “MULTIPLE TUMOR & INFECTION DETECTION IN MRI BRAIN IMAGE USING SVM CLASSIFIER”, (International Conference on Engineering and Technology Systems, Pak. J. Biotechnol. Vol. 13 special issue II, Pp. 101 - 105 (2016).
- [2] J. Amin et al., A distinctive approach in brain tumor detection and classification using MRI, Pattern Recognition Letters (2017), <https://doi.org/10.1016/j.patrec.2017.10.036>
- [3] S. K. Shil et. al. “An improved brain tumor detection and classification mechanism”, IEEE, 2017.
- [4] V. Shreyas, and Vinod Pankajakshan, “A Deep Learning Architecture for Brain Tumor Segmentation in MRI Images”, IEEE, 2017.
- [5] Mohamed Babikir Ali et. al. “Optimizing Convolutional Neural Networks for Brain Tumor Segmentation in MRI Images”, International Conference on Computer, Control, Electrical, and Electronics Engineering (ICCCEEE), IEEE, 2018.
- [6] Tonmoy Hossain et. al. “Brain Tumor Detection Using Convolutional Neural Network”, 1st International Conference on Advances in Science, Engineering and Robotics Technology 2019 (ICASERT 2019), IEEE, 2019.
- [7] Mustafa R. Ismael and Ikhlas Abdel-Qader, “Brain Tumor Classification via Statistical Features and Back-Propagation Neural Network”, IEEE, 2018.
- [8] Milica M. Badza and Marko C. Barjaktarovic, “Classification of Brain Tumors from MRI Images Using a Convolutional Neural Network”, Appl. Sci. 2020, 10, 1999; doi:10.3390/app10061999.
- [9] Pratima Purushottam Gumaste and Vinayak K. Bairagi, “A Hybrid Method for Brain Tumor Detection using Advanced Textural Feature Extraction”, Biomedical & Pharmacology Journal, Vol. 13(1), p. 145-157, March 2020.
- [10] Bala Venkateswarlu Isunuri and Jagadeesh Kakarla, “Fast brain tumor segmentation using optimized U-Net and adaptive thresholding”, Automatika, Taylor and Francis, 61:3, 352-360, DOI: 10.1080/00051144.2020.1760590.
- [11] Mohamed Nasor and Walid Obaid, “Detection and Localization of Early-Stage Multiple Brain Tumors Using a Hybrid Technique of Patch-Based Processing, k-means Clustering and Object

- Counting”, *International Journal of Biomedical Imaging*, Hindawi, Volume 2020, <https://doi.org/10.1155/2020/9035096>.
- [12] Muhammad Sharif et. al., “Brain tumor detection based on extreme learning”, *Neural Computing and Applications*, Springer, <https://doi.org/10.1007/s00521-019-04679-8>, 2020.
- [13] Shargunam S and Gopika Rani N, “Detection of Brain Tumor in Medical Imaging”, 6th International conference on advanced computing and communication systems (ICACCS), IEEE, 2020.
- [14] Suresha D et. al., “Detection of Brain Tumor Using Image Processing”, e Fourth International Conference on Computing Methodologies and Communication (ICCMC 2020), IEEE, 2020.
- [15] Ayoub Adineh-vand, Gholamreza Karimi and Mozafar Khazaei, “A Hierarchical Convolutional Neural Network Architecture for Brain Tumor Segmentation in 3D Brain Magnetic Resonance Imaging”, *Multidisciplinary Cancer Investigation*, Volume 4, Issue 1, January 2020.
- [16] Ahmet Çinar and Muhammed Yildirim , “Detection of tumors on brain MRI images using the hybrid convolutional neural network architecture”, Elsevier 2020, <https://doi.org/10.1016/j.mehy.2020.109684>.
- [17] Muhammad Waqas Nadeem et. al., “Brain Tumor Analysis Empowered with Deep Learning: A Review, Taxonomy, and Future Challenges”, *Brain Sci.* 2020, 10, 118; doi:10.3390/brainsci10020118.
- [18] C.Hemasundara Rao et al. “Brain tumor detection and segmentation using conditional random field”, 7th International Advance Computing Conference, IEEE 2017